

# Deep ultraviolet photoconductive and near-infrared luminescence properties of Er<sup>3+</sup>-doped $\beta$ -Ga<sub>2</sub>O<sub>3</sub> thin films

Cite as: Appl. Phys. Lett. **108**, 211903 (2016); <https://doi.org/10.1063/1.4952618>

Submitted: 01 April 2016 . Accepted: 12 May 2016 . Published Online: 24 May 2016

Zhenping Wu, Gongxun Bai, Yingyu Qu, Daoyou Guo, Linghong Li, Peigang Li, Jianhua Hao, and Weihua Tang



View Online



Export Citation



CrossMark

## ARTICLES YOU MAY BE INTERESTED IN

[A review of Ga<sub>2</sub>O<sub>3</sub> materials, processing, and devices](#)

Applied Physics Reviews **5**, 011301 (2018); <https://doi.org/10.1063/1.5006941>

[Oxygen vacancy tuned Ohmic-Schottky conversion for enhanced performance in  \$\beta\$ -Ga<sub>2</sub>O<sub>3</sub> solar-blind ultraviolet photodetectors](#)

Applied Physics Letters **105**, 023507 (2014); <https://doi.org/10.1063/1.4890524>

[High responsivity in molecular beam epitaxy grown  \$\beta\$ -Ga<sub>2</sub>O<sub>3</sub> metal semiconductor metal solar blind deep-UV photodetector](#)

Applied Physics Letters **110**, 221107 (2017); <https://doi.org/10.1063/1.4984904>

Lock-in Amplifiers  
Find out more today



Zurich  
Instruments

# Deep ultraviolet photoconductive and near-infrared luminescence properties of Er<sup>3+</sup>-doped $\beta$ -Ga<sub>2</sub>O<sub>3</sub> thin films

Zhenping Wu,<sup>1,2,3</sup> Gongxun Bai,<sup>4,5</sup> Yingyu Qu,<sup>1</sup> Daoyou Guo,<sup>1</sup> Linghong Li,<sup>6</sup> Peigang Li,<sup>1,7</sup> Jianhua Hao,<sup>4,5,a)</sup> and Weihua Tang<sup>1,2,a)</sup>

<sup>1</sup>Laboratory of Optoelectronics Materials and Devices, School of Science, Beijing University of Posts and Telecommunications, Beijing 100876, China

<sup>2</sup>State Key Laboratory of Information Photonics and Optical Communications, Beijing University of Posts and Telecommunications, Beijing 100876, China

<sup>3</sup>Department of Quantum Matter Physics, University of Geneva, 24 Quai Ernest-Ansermet, 1211 Geneva, Switzerland

<sup>4</sup>Department of Applied Physics, The Hong Kong Polytechnic University, Hong Kong, China

<sup>5</sup>The Hong Kong Polytechnic University Shenzhen Research Institute, Shenzhen 518057, China

<sup>6</sup>Department of Physics, The State University of New York at Potsdam, Potsdam, New York 13676-2294, USA

<sup>7</sup>Center for Optoelectronics Materials and Devices, Department of Physics, Zhejiang Sci-Tech University, Hangzhou 310018, Zhejiang, China

(Received 1 April 2016; accepted 12 May 2016; published online 24 May 2016)

Highly oriented ( $\bar{2}01$ ) Er<sup>3+</sup>-doped  $\beta$ -Ga<sub>2</sub>O<sub>3</sub> (Er:Ga<sub>2</sub>O<sub>3</sub>) thin films with different doping concentrations were grown on (0001) sapphire substrates using radio frequency magnetron sputtering. The crystal structure, optical absorption, near-infrared luminescence, and ultraviolet photoresponse properties of Er:Ga<sub>2</sub>O<sub>3</sub> films were systematically studied. The evolution of lattice and energy band gap with increasing doping level confirms the chemical substitution of Er<sup>3+</sup> ions into the Ga<sub>2</sub>O<sub>3</sub> crystal lattice. The down-shifting near-infrared luminescence ( $\sim 1538$  nm; ascribed to Er<sup>3+</sup>: <sup>4</sup>I<sub>13/2</sub>—<sup>4</sup>I<sub>15/2</sub>) was observed under ultraviolet excitation. Moreover, an obvious deep ultraviolet photoresponse was also obtained in the formed thin films. *Published by AIP Publishing.*

[<http://dx.doi.org/10.1063/1.4952618>]

Recently, deep ultraviolet (DUV) photodetectors have attracted intensive interest for the development of civil and military surveillance applications, such as chemical/biological analysis, missile tracking, secure communication, ozone holes monitoring, and so on.<sup>1–4</sup> One of the notable features of a DUV photodetector is the detection accuracy of very weak signals because of the “black background” on earth, where wavelengths shorter than 280 nm are absent in solar radiation and artificial light. During the past decade, several materials—such as AlGa<sub>2</sub>N, ZnMgO, diamond, and  $\beta$ -Ga<sub>2</sub>O<sub>3</sub>—with a wide bandgap ( $>4.4$  eV) have been employed to fabricate DUV photodetectors.<sup>3–7</sup> Among them, as a transparent semiconductor with a band gap of  $\sim 4.9$  eV, monoclinic  $\beta$ -Ga<sub>2</sub>O<sub>3</sub> (space group: C2/m) with the lattice parameters of  $a = 12.23$  Å,  $b = 3.04$  Å,  $c = 5.80$  Å, and  $\beta = 103.7^\circ$  has been considered as one of the ideal candidates for DUV photodetectors. Previous studies indicate that  $\beta$ -Ga<sub>2</sub>O<sub>3</sub> based metal-semiconductor-metal (MSM) and  $p$ - $n$  junction structure photodetectors show both easy growth and high responsivity characteristics.<sup>3,4,7–10</sup>

Moreover, as a highly thermally and chemically stable wide bandgap semiconductor,  $\beta$ -Ga<sub>2</sub>O<sub>3</sub> is also the ideal host material for lanthanide ions, which could introduce additional energy transitions.<sup>11,12</sup> Great efforts have been made to investigate the luminescence from lanthanide-doped materials for a wide range of applications, including optoelectronic devices and biomedicine and optical waveguides, especially in the near-infrared (NIR) region where optical communication systems operate.<sup>13–16</sup> For instance, by embedding lanthanide ions

such as neodymium into  $\beta$ -Ga<sub>2</sub>O<sub>3</sub> thin films, an enhanced UV to NIR down-shifting luminescence is observed.<sup>16</sup> In this direction, it could be a promising approach to fabricate a sensitive photoluminescence (PL)-detecting sensor based on lanthanide-doped  $\beta$ -Ga<sub>2</sub>O<sub>3</sub>.<sup>17</sup> Therefore, it would be very attractive if the DUV light source could generate both electric and luminescence signals, offering a dual-mode functional detection.

Here, we report the fabrication of Er<sup>3+</sup> doped  $\beta$ -Ga<sub>2</sub>O<sub>3</sub> films grown on sapphire substrates and the characteristics of their NIR luminescence and ultraviolet photoresponse. The utilization of a thin-film structure would be beneficial in terms of increasing device reproducibility, owing to the available well established thin-film fabrication technologies. Additionally, the integration of ultraviolet photoconductive and NIR luminescence on a single wafer will be very helpful in developing a potential hybrid system for a high performance DUV photodetector. Figure 1(a) shows the schematic configuration of ultraviolet photoelectric and NIR luminescence in Er:Ga<sub>2</sub>O<sub>3</sub> films. As a commonly used phosphor, Erbium is selected as the dopant for investigating the near-infrared luminescence. Particularly interesting is the 1.55  $\mu$ m emission of Er<sup>3+</sup>, which corresponds to the wavelength of minimal optical loss in silica-based optical fibers.<sup>12,18,19</sup> The monoclinic-structure Er<sup>3+</sup> doped  $\beta$ -Ga<sub>2</sub>O<sub>3</sub> can also possess a non-centrosymmetric structure and inherently exhibit PL characteristics.

Er:Ga<sub>2</sub>O<sub>3</sub> films were deposited on top of (0001) oriented single crystal Al<sub>2</sub>O<sub>3</sub> (10 mm  $\times$  10 mm  $\times$  0.5 mm) by radio frequency magnetron sputtering. Several high purity Er<sub>2</sub>O<sub>3</sub> strips were embedded into the Ga<sub>2</sub>O<sub>3</sub> target to control the doping concentration. The base pressure in the sputtering

<sup>a)</sup>Authors to whom correspondence should be addressed. Electronic addresses: jh.hao@polyu.edu.hk and whtang@bupt.edu.cn

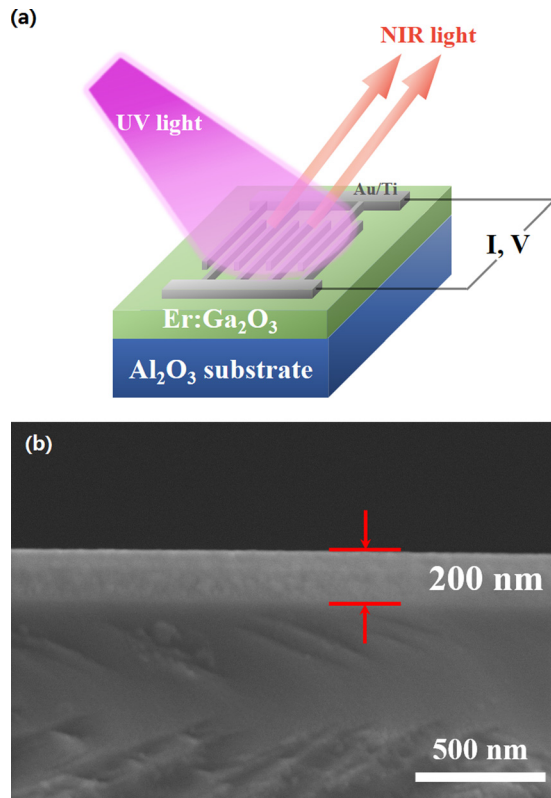


FIG. 1. (a) The setup used for measuring the near-infrared luminescent and photocurrent of Er:Ga<sub>2</sub>O<sub>3</sub> film grown on sapphire substrate under a ultraviolet light. (b) Cross-sectional SEM image for the as-grown Er:Ga<sub>2</sub>O<sub>3</sub> film.

chamber was  $1 \times 10^{-4}$  Pa. The growth temperature ranged from 550 °C to 800 °C. The gas pressure (Ar:O<sub>2</sub> = 2:1) was fixed at 1 Pa. The thickness of the films was about 200 nm, confirmed by the scanning electron microscope results (as shown in Figure 1(b)). After the deposition, *in-situ* post-annealing in a 200 mbar oxygen pressure for 60 min was used to fill oxygen vacancies formed during growth. The PL spectra were recorded using an Edinburgh FLSP920 spectrophotometer under the excitation of a Xeon lamp (~450 W). NIR PL spectra were detected with a nitrogen-cooled NIR photomultiplier tube (Hamamatsu C9940-02). The current-voltage (I-V) and time-dependent photoresponse were measured by a Keithly 2400. An ultraviolet (UV) lamp (~7 W) with a wavelength of 254 nm was employed as the light source for the UV response measurement. All the characterizations were carried out at room temperature.

The crystal structure characterization was performed *ex-situ* with a Bruker D8 Advance X-ray diffractometer (using Cu K- $\alpha_1$  radiation,  $\lambda = 1.5406$  Å). Figure 2(a) displays the  $\theta$ - $2\theta$  scans of the Ga<sub>2</sub>O<sub>3</sub> thin films deposited at various substrate temperatures. When the growth temperature is below 600 °C, no peaks appear except for Al<sub>2</sub>O<sub>3</sub>-related diffraction peaks, implying that there might not be enough kinetic energy for the formation of  $\beta$ -Ga<sub>2</sub>O<sub>3</sub> films. When the substrate temperature is between 650 °C and 750 °C, three peaks located at 18.83°, 38.17°, and 58.86° corresponding to  $\beta$ -Ga<sub>2</sub>O<sub>3</sub> ( $\bar{2}01$ ), ( $\bar{4}02$ ), and ( $\bar{6}03$ ) are observed, in addition to the diffraction peak of the substrate. When the substrate temperature is up to 800 °C, extra diffraction peaks of (110), ( $\bar{3}13$ ), and (113) of Ga<sub>2</sub>O<sub>3</sub> phase appear. Moreover, the

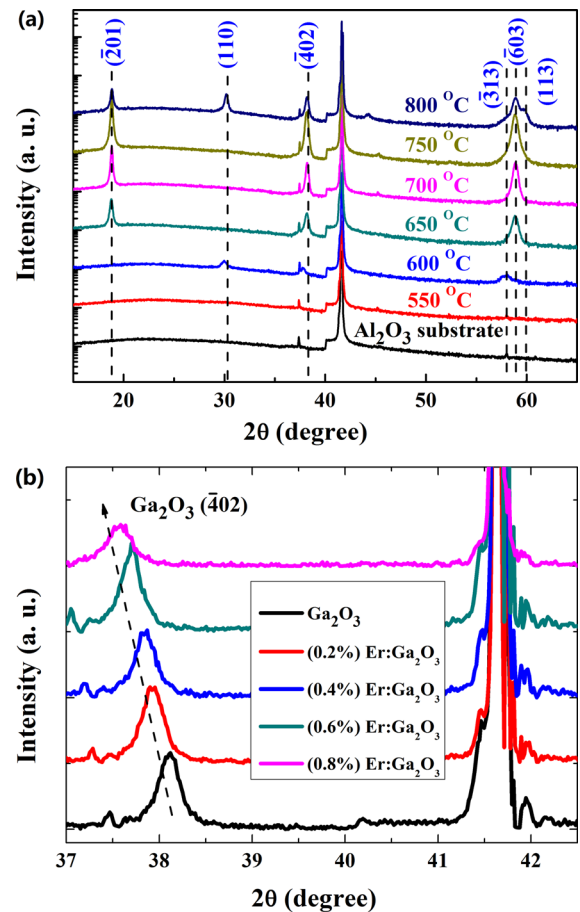


FIG. 2. (a) XRD patterns of the Ga<sub>2</sub>O<sub>3</sub> thin films deposited at various substrate temperatures. (b)  $\theta$ - $2\theta$  spectrum in a narrow range of the Er:Ga<sub>2</sub>O<sub>3</sub> films with different doping concentration level (0%, 0.2 mol. %, 0.4 mol. %, 0.6 mol. %, and 0.8 mol. %).

intensity of the peak corresponding to the Ga<sub>2</sub>O<sub>3</sub> ( $\bar{2}01$ ) phase decreases, indicating a polycrystalline nature. As a result, optimal deposition conditions were found to be at a substrate temperature of 750 °C.

Using the optimized parameter, undoped  $\beta$ -Ga<sub>2</sub>O<sub>3</sub> and Er:Ga<sub>2</sub>O<sub>3</sub> epitaxial thin films were fabricated. For both the Ga<sub>2</sub>O<sub>3</sub> and Er:Ga<sub>2</sub>O<sub>3</sub> films, only the ( $\bar{2}01$ ) peak and higher order peaks of the monoclinic  $\beta$  phase are present, which indicates that the films are grown with a preferred ( $\bar{2}01$ ) plane orientation [Figure 2(b)]. The Er doping concentrations were determined as 0.2 mol. %, 0.4 mol. %, 0.6 mol. %, and 0.8 mol. % by the X-ray photoelectron spectroscopy (XPS), respectively. As clearly seen from the XRD patterns, a remarkable structural modification is induced by the Er doping. For the Er:Ga<sub>2</sub>O<sub>3</sub> thin films, the positions of the ( $\bar{4}02$ ) peaks gradually shift to lower  $2\theta$  compared to the undoped Ga<sub>2</sub>O<sub>3</sub> thin film. The shift in the  $2\theta$  values indicates an increase of the lattice constants, which can be attributed to the ionic radii difference (~30%) between Er<sup>3+</sup> and Ga<sup>3+</sup> (Er<sup>3+</sup>: 0.89 Å, Ga<sup>3+</sup>: 0.62 Å for octahedral coordination and 0.47 Å for tetrahedral coordination, respectively).<sup>20</sup> Moreover, a comparison of the XRD patterns with various Er<sup>3+</sup> doping shows broader and lower intensity diffraction peaks for samples with higher Er<sup>3+</sup> doping concentrations, which suggests that higher concentrations may lead to the worse crystallinity.

Figure 3(a) gives the ultraviolet-visible (UV-Vis) absorbance spectrum of Er:Ga<sub>2</sub>O<sub>3</sub> and pure Ga<sub>2</sub>O<sub>3</sub> at room temperature. The spectra of the measured samples exhibit a sharp absorption edge at wavelengths between 250 nm and 270 nm. It indicates that the obtained Er:Ga<sub>2</sub>O<sub>3</sub> thin films are highly transparent to light with wavelengths above 280 nm, confirming a suitable candidate for a solar-blind photodetector. The band gap is fitted by extrapolating the linear region of the plot  $(\alpha h\nu)^2$  versus  $h\nu$ , as shown in the inset of Figure 3(a), where  $h$  is Planck's constant,  $\alpha$  is the linear absorption coefficient, and  $\nu$  is the transition frequency of incident photon. For 0.2 mol. % doped Er:Ga<sub>2</sub>O<sub>3</sub>, the band gap decreased slightly from 4.95 eV to 4.82 eV. Such a band gap reduction phenomenon could be due to unoccupied in-gap states in Ga<sub>2</sub>O<sub>3</sub> by Er<sup>3+</sup> ions substitution. However, as the doping concentration increases further, the gap is then gradually increased to 5 eV. The observed broadening of the band gap can be attributed to the reduced crystalline quality, which is consistent with the XRD results.

Figure 3(b) shows the NIR region PL spectra of Er:Ga<sub>2</sub>O<sub>3</sub> with excitation at 254 nm by Xeon lamp. The typical one band NIR PL emission located at 1538 nm is attributed to the erbium transition  $^4I_{13/2} \rightarrow ^4I_{15/2}$ . As seen, the emission intensity can be remarkably enhanced with increasing Er<sup>3+</sup> doping concentration. The most probable site for the Er<sup>3+</sup> ions substitution is at the distorted octahedral sites of the

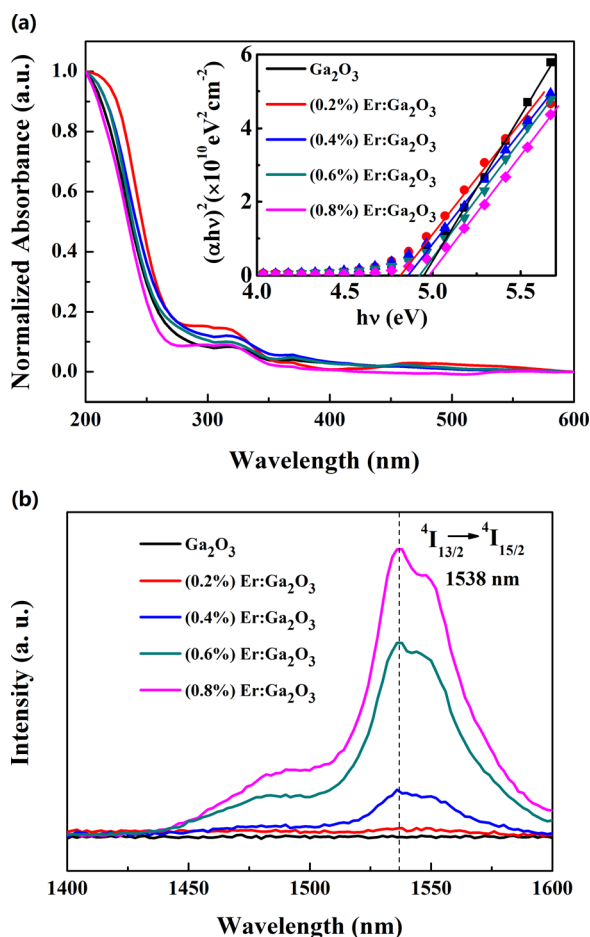


FIG. 3. (a) Absorption spectra of Er:Ga<sub>2</sub>O<sub>3</sub> thin films compared with that of pure  $\beta$ -Ga<sub>2</sub>O<sub>3</sub> thin film and the plot of  $(\alpha h\nu)^2$  versus  $h\nu$  in inset. (b) NIR Photoluminescence spectra of Er:Ga<sub>2</sub>O<sub>3</sub> films with different concentrations.

Ga<sub>2</sub>O<sub>3</sub> lattice with an inversion center, which implies the selection rules forbidding all 4f–4f electric dipole (ED) transitions. When the dopant concentration increases, the elongation of the d spacing of (201) plane promotes the structure asymmetry of the Ga<sub>2</sub>O<sub>3</sub> host, approaching lower symmetry around Er<sup>3+</sup> ions. In principle, the lower symmetry means that the more uneven crystal-field components can mix opposite-parity into 4f levels and subsequently increase the ED transition probabilities of the dopant ions, resulting in the enhancement of NIR PL emission. The above-mentioned results demonstrate the existence of efficient energy transfer (ET) from the electron-hole pairs created in the Ga<sub>2</sub>O<sub>3</sub> host to the Er<sup>3+</sup> ions. In this process, the Ga<sub>2</sub>O<sub>3</sub> will act as an effective light harvester to absorb UV photons and subsequently transfer energy to Er<sup>3+</sup> ion, thereby resulting in the typical NIR luminescence.

To evaluate the UV photoconductance, interdigital Ti/Au electrodes were deposited on top of the Er:Ga<sub>2</sub>O<sub>3</sub> thin films using a shadow mask to construct a MSM structure prototype device. The electrode fingers were 100  $\mu$ m wide, 2800  $\mu$ m long, and 100  $\mu$ m spacing gap. The effective irradiated area was  $\sim 0.021$  cm<sup>2</sup>. Figure 4(a) shows the I-V characteristic curves of the 0.8 mol. % Er:Ga<sub>2</sub>O<sub>3</sub> thin film based MSM photodetectors under the light sources with the wavelengths of 365 nm and 254 nm. It can be seen clearly that the current increases linearly as the applied bias increases both in dark

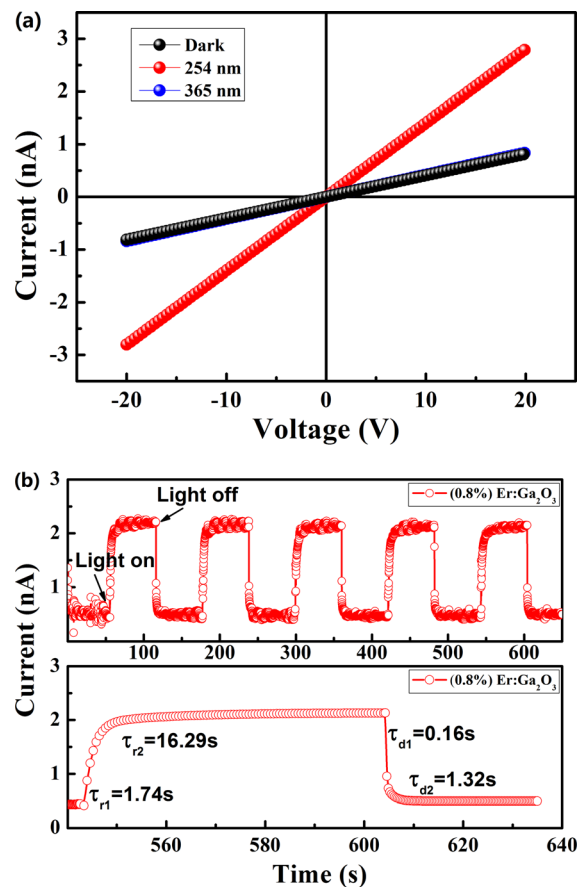


FIG. 4. (a) The I-V curves of the 0.8 mol. % Er:Ga<sub>2</sub>O<sub>3</sub> photodetector in dark and under the light sources with the wavelength of 254 nm and 365 nm. (b) Time-dependent photoresponse of the 0.8 mol. % Er:Ga<sub>2</sub>O<sub>3</sub> thin film to 254 nm illumination (up), enlarged view of the rise/decay edges and the corresponding exponential fitting for the devices (down).

and under different illumination. The fresh dark current is about 0.8 nA at a voltage of 20 V. The I-V curve under 365 nm light does not show significant increase as compared with the I-V curve in dark, which suggests the Er:Ga<sub>2</sub>O<sub>3</sub> thin films are not sensitive to 365 nm light. When the photodetectors are exposed to the 254 nm light, the slopes of I-V curves show a sharp increase. The sensitivity of the photodetector, defined as  $(I_{il}-I_d)/I_d$  in percent ( $I_{il}$  is the current of the device when illuminated with a light source and  $I_d$  is the dark current), is approximately as high as 2.5, suggesting a good application in ultraviolet photodetectors.<sup>21</sup> Another important parameter for a UV photodetector is response time. Figure 4(b) (top) shows the time-dependent photoresponse of the detector to 254 nm illumination by on/off switching under an applied bias of 15 V. For the time-dependent photoresponse, the device still exhibits a nearly identical response after multiple illumination cycles, indicating the high robustness and good reproducibility of the photodetectors. The quantitative analysis of the current rise and decay process involves the fitting of the photoresponse curve with a bi-exponential relaxation equation of the following type:  $I = I_0 + Ae^{-t/\tau_1} + Be^{-t/\tau_2}$ , where  $I_0$  is the steady state photocurrent,  $t$  is time, A and B are constants, and  $\tau_1$  and  $\tau_2$  are two relaxation time constants.<sup>22</sup> The response (rise) edges and recovery (decay) edges usually consist of two components with a fast-response component and a slow-response component. Generally, the fast-response component can be attributed to the rapid change of carrier concentration as soon as the light is turned on/off, while the slow-response component is caused by the carrier trapping/releasing owing to the existence of defects in the thin films. For Er:Ga<sub>2</sub>O<sub>3</sub> thin films, the rise time constant and decay time constant of Er:Ga<sub>2</sub>O<sub>3</sub> 0.8% are estimated to be 1.74 s/16.29 s and 0.16 s/1.32 s, respectively [as shown in Fig. 4(b) bottom]. Compared to our previous works, the obtained sensitivity is slightly smaller with a comparable response speed. There might be two possible reasons for this: first, with the Er<sup>3+</sup> doping concentration increasing, the worse crystallinity could generate more trapping states, which could capture the photogenerated carriers; second, part of the released energy due to the recombination of electrons with the photogenerated holes is transferred to the excited states of the Er<sup>3+</sup> ions.

In summary, we have demonstrated DUV illumination with both NIR down-shifting PL and photoconductive in Er<sup>3+</sup> doped  $\beta$ -Ga<sub>2</sub>O<sub>3</sub> thin films. Erbium doping was verified by XRD and UV-Vis absorbance spectrum results. The enhanced NIR luminescence observation was associated with the lattice distortion and crystal field variation in

Er:Ga<sub>2</sub>O<sub>3</sub>. The detailed photoelectrical characteristics of an MSM structured photodetector were also investigated. Our results may offer great potential in developing a dual-modal DUV photodetector combining photoconductive and NIR luminescence for a variety of applications.

This work was supported by the National Natural Science Foundation of China (Nos. 11404029, 51572033, 61274017, 51572241, and 51272218), Beijing Natural Science Foundation (No. 2154055), Fund of State Key Laboratory of Information Photonics and Optical Communications (BUPT), and the Fundamental Research Funds for the Central Universities (Grant No. 2014RC0906).

- <sup>1</sup>P. Y. Fan, U. K. Chettiar, L. Y. Cao, F. Afshinmanesh, N. Engheta, and M. L. Brongersma, *Nat. Photonics* **6**, 380–385 (2012).
- <sup>2</sup>S. M. Hatch, J. Briscoe, and S. Dunn, *Adv. Mater.* **25**, 867–871 (2013).
- <sup>3</sup>Y. Li, T. Tokizono, M. Liao, M. Zhong, Y. Koide, I. Yamada, and J.-J. Delaunay, *Adv. Funct. Mater.* **20**, 3972 (2010).
- <sup>4</sup>W. Feng, X. Wang, J. Zhang, L. Wang, W. Zheng, P. Hu, W. Cao, and B. Yang, *J. Mater. Chem. C* **2**, 3254 (2014).
- <sup>5</sup>Y. Zhao, J. Zhang, D. Jiang, C. Shan, Z. Zhang, B. Yao, D. Zhao, and D. Shen, *ACS Appl. Mater. Interfaces* **1**, 2428 (2009).
- <sup>6</sup>G. Bao, D. Li, X. Sun, M. Jiang, Z. Li, H. Song, H. Jiang, Y. Chen, G. Miao, and Z. Zhang, *Opt. Express* **22**, 24286 (2014).
- <sup>7</sup>D. Y. Guo, Z. P. Wu, Y. H. An, X. C. Guo, X. L. Chu, C. L. Sun, L. H. Li, P. G. Li, and W. H. Tang, *Appl. Phys. Lett.* **105**, 023507 (2014).
- <sup>8</sup>D. Y. Guo, Z. P. Wu, P. G. Li, Y. H. An, H. Liu, X. C. Guo, H. Yan, G. F. Wang, C. L. Sun, L. H. Li, and W. H. Tang, *Opt. Mater. Express* **4**, 1067 (2014).
- <sup>9</sup>X. C. Guo, N. H. Hao, D. Y. Guo, Z. P. Wu, Y. H. An, X. L. Chu, L. H. Li, P. G. Li, M. Lei, and W. H. Tang, *J. Alloys Compd.* **660**, 136–140 (2016).
- <sup>10</sup>Y. Teng, L. X. Song, A. Ponchel, Z. K. Yang, and J. Xia, *Adv. Mater.* **26**(36), 6238–6243 (2014).
- <sup>11</sup>P. N. Favennec, H. Lharidon, M. Salvi, D. Moutonnet, and Y. Leguillou, *Electron. Lett.* **25**, 718–719 (1989).
- <sup>12</sup>J. Hao, Z. Lou, I. Renaud, and M. Cocivera, *Thin Solid Films* **467**(1), 182–185 (2004).
- <sup>13</sup>D. T. Tu, L. Q. Liu, Q. Ju, H. M. Zhu, R. F. Li, and X. Y. Chen, *Angew. Chem., Int. Ed.* **50**, 6306–6310 (2011).
- <sup>14</sup>G. X. Bai, M. K. Tsang, and J. H. Hao, *Adv. Opt. Mater.* **3**, 416 (2015).
- <sup>15</sup>Z. P. Wu, G. X. Bai, Q. R. Hu, D. Y. Guo, C. L. Sun, L. Y. Ji, M. Lei, L. H. Li, P. G. Li, J. H. Hao, and W. H. Tang, *Appl. Phys. Lett.* **106**, 171910 (2015).
- <sup>16</sup>Y. Zhang and J. Hao, *J. Mater. Chem. C* **1**(36), 5607–5618 (2013).
- <sup>17</sup>Z. Zhou, R. Shinar, A. J. Allison, and J. Shinar, *Adv. Funct. Mater.* **17**, 3530 (2007).
- <sup>18</sup>A. J. Kenyon, *Prog. Quantum Electron.* **26**, 225–284 (2002).
- <sup>19</sup>J. Hao and M. Cocivera, *J. Phys. D: Appl. Phys.* **35**(5), 433 (2002).
- <sup>20</sup>R. D. Shannon, *Acta Crystallogr., Sect. A* **32**, 751–767 (1976).
- <sup>21</sup>W. Tian, C. Zhi, T. Zhai, S. Chen, X. Wang, M. Liao, D. Golberg, and Y. Bando, *J. Mater. Chem.* **22**, 17984 (2012).
- <sup>22</sup>N. Liu, G. Fang, W. Zeng, H. Zhou, F. Cheng, Q. Zheng, L. Yuan, X. Zou, and X. Zhao, *ACS Appl. Mater. Interfaces* **2**, 1973 (2010).